



# Controlled synthesis of nanostructured Co film catalysts with high performance for hydrogen generation from sodium borohydride solution

Hao Li<sup>a,b,\*\*</sup>, Jinyun Liao<sup>a</sup>, Xibin Zhang<sup>a</sup>, Weiwen Liao<sup>a</sup>, Lili Wen<sup>a</sup>, Jingbo Yang<sup>a</sup>, Hui Wang<sup>c</sup>, Rongfang Wang<sup>b,c,\*</sup>

<sup>a</sup> Department of Chemical Engineering, Huizhou University, Huizhou 516007, PR China

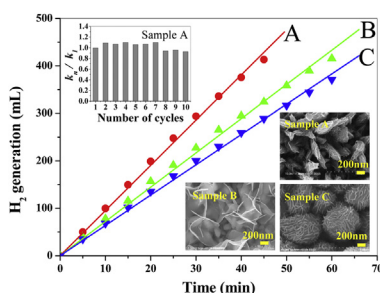
<sup>b</sup> Key Laboratory of Fuel Cell Technology of Guangdong Province, Guangzhou 510641, PR China

<sup>c</sup> Key Laboratory of Eco-Environment-Related Polymer Materials, Ministry of Education of China, College of Chemistry and Chemical Engineering, Northwest Normal University, Lanzhou 730070, PR China

## HIGHLIGHTS

- Novel Co films are prepared by a magnetic-field-induced deposition route.
- The Co film catalysts exhibit high performance in the hydrolysis of NaBH<sub>4</sub>.
- The Co nanostructures are crucial for their high catalytic activity.

## GRAPHICAL ABSTRACT



## ARTICLE INFO

### Article history:

Received 24 January 2013

Received in revised form

24 March 2013

Accepted 27 March 2013

Available online 8 April 2013

### Keywords:

Nanostructure

Catalysts

Co film

Hydrogen generation

Controlled synthesis

## ABSTRACT

As a representative catalyst for the hydrolysis of NaBH<sub>4</sub> to produce hydrogen, nanostructured Co has received intensive attention owing to its high catalytic activity and low cost. In this study, nanostructured Co films supported on Cu foils are fabricated by a facile and cost effective magnetic-field-induced chemical reduction method. By controlling the synthetic conditions, Co films composed of nanoplatelets, nanosheets and microspheres are successfully obtained. It is found that the as-prepared nanostructured Co film catalysts exhibit high performance in the hydrolysis of sodium borohydride. The rate constant/apparent activation energy of NaBH<sub>4</sub> hydrolysis in the presence of these Co film catalysts is 1.27 mL min<sup>-1</sup> cm<sup>-2</sup>/28.4 kJ mol<sup>-1</sup>, 0.96 mL min<sup>-1</sup> cm<sup>-2</sup>/27.6 kJ mol<sup>-1</sup> and 0.85 mL min<sup>-1</sup> cm<sup>-2</sup>/34.3 kJ mol<sup>-1</sup>, respectively. Interestingly, Co film composed of nanoplatelets shows only ca. 10% catalytic activity loss after 10 cycles, which exhibits much improved reusability and durability in contrast to those Co catalysts reported in the literature.

© 2013 Elsevier B.V. All rights reserved.

## 1. Introduction

The worldwide energy consumption is rapidly growing and the current energy system based on fossil fuels is the major cause of global climate change and environmental pollution, which makes it an urgent task to search for clean and sustainable energy source [1,2]. Owing to its high energy density, zero emission and abundant

\* Corresponding author. Key Laboratory of Fuel Cell Technology of Guangdong Province, Guangzhou 510641, PR China. Tel./fax: +86 931 7971533.

\*\* Corresponding author. Department of Chemical Engineering, Huizhou University, Huizhou 516007, PR China. Tel./fax: +86 752 2527229.

E-mail addresses: [lihao180@126.com](mailto:lihao180@126.com) (H. Li), [wrf38745779@126.com](mailto:wrf38745779@126.com), [wangrf@nwnu.edu.cn](mailto:wangrf@nwnu.edu.cn) (R. Wang).

source, hydrogen is envisioned as the next-generation fuel in the field of transportation and even personal electronics. However, before the large-scale application of hydrogen, the problem of the hydrogen storage and delivery resulted from the fact that hydrogen is gas with extremely low density ( $8.9 \times 10^{-5} \text{ g cm}^{-3}$ ) at room temperature should be resolved [3,4]. Currently,  $\text{NaBH}_4$  is widely accepted as a promising material to store and delivery hydrogen in view of its multi-advantages, including high hydrogen content of 10.8 wt%, relatively high stability in solid state and solution, commercially availability with low cost, non-toxicity [5,6]. Though the hydrolysis of  $\text{NaBH}_4$  at room temperature is spontaneous, the hydrogen generation rate is quite low and will decrease as the reaction proceeds due to an increase of pH value of the solution caused by the formation of borates. Therefore, the utilization of catalyst is indispensable in order to accelerate the hydrolysis reaction.

It has been reported that acids, noble metals, transition metals/alloys or metal salts can effectively catalyze  $\text{NaBH}_4$  hydrolysis [4,5,7,8]. Among these catalysts, Co-based nanocatalysts have drawn special attention on account of their high catalytic performance and much lower cost compared with noble metal nanoparticle catalysts. Recently, production of hydrogen from  $\text{NaBH}_4$  hydrolysis catalyzed by powdery Co-based nanocatalysts under different reaction conditions has been well documented [9–14]. However, supported or unsupported magnetic nanoparticles in the form of powder are likely to aggregate owing to their high surface energy and magnetic attraction between each other, which may lower their catalytic activity and reduce the lifetime of catalyst [15,16]. Moreover, the tedious and costly separation and recovery procedure of these powdery nanocatalysts is another challenge when these catalysts are in industry-scale application. In contrast, Co nanocatalysts in the form of film are easy to recover and reuse, stable, which make it more attractive in the  $\text{NaBH}_4$  hydrolysis [17–19].

On the other hand, the catalytic activity of many nanomaterials is sensitively dependent on their morphology and architectures. For instance, compared to the spherical nanocatalysts, those shape-anisotropic nanocatalysts with more edges, corners and faces can provide more active site for catalytic reaction, which will exhibit much higher catalytic performance in many cases [20–23]. In this regard, nanostructured Co films consisting of shape-anisotropic nano-units are expected to show better catalytic activity in the  $\text{NaBH}_4$  hydrolysis than those traditional Co films composed of Co nanoparticles. However, in spite of significant advances in the synthetic process of metal film, fabrication of Co film composed of shape-anisotropic Co nanocrystals with uniform and novel morphology is still a big challenge and has been rarely reported [17,24–28].

In this study, we report a facile and cost-effective magnetic-field-assisted deposition process to synthesize nanostructured Co films, in which magnetic Co units formed in solution by chemical reduction were transferred to the Cu foil supports and then deposited on the supports under the induction of an external magnetic field. It is found that nanostructured Co films comprised of shape-anisotropic Co nanocrystals, such as Co nanoplatelets, Co

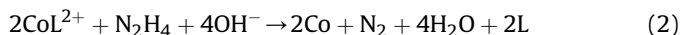
nanosheets, and Co microspheres composed of nanosheets, could be successfully prepared by controlling the reaction conditions. Compared with those common Co films consisting of small spherical Co grains, the as-prepared Co films display novel nano-architectures. To the best of our knowledge, similar nanostructured Co films used as catalysts for  $\text{NaBH}_4$  hydrolysis have not been reported. More importantly, it is found that these Co film catalysts exhibit relatively high catalytic performance in the hydrolysis reaction of  $\text{NaBH}_4$  in contrast to the recently reported Co film catalysts in the literature.

## 2. Experimental section

### 2.1. Synthesis

All reagents were of analytic grade, and double-distilled water was used throughout the experiments. To prepare nanostructured Co film supported on foil (sample A), 2 mmol  $\text{CoCl}_2 \cdot 6\text{H}_2\text{O}$  was dissolved into 20 mL water under intense stirring, followed by addition of 4 mmol triethylene tetramine to the  $\text{CoCl}_2$  solution. Then, 10 mL NaOH (10 mol/L), 10 mL hydrazine hydrate solution (50%) and 40 mL ethanol were dropped in sequence to the above solution, resulting in a final solution of ca. 80 mL. Afterward, the solution was transferred into a teflon-lined steel autoclave, in which a piece of  $5 \times 12 \text{ cm}$  Cu foil with a thickness of ca. 10  $\mu\text{m}$  and a weight of  $0.54 \pm 0.02 \text{ g}$  (obtained from Guangzhou Great Power Energy & Technology CO, LTD) closely attached to the inner wall of vessel was used as support. Then the autoclave was put in the center of a circular column magnet with the magnetic field intensity of ca. 0.2 T around the inner wall of the vessel. Finally, the autoclave, together with the magnet, was kept in an oven at 100  $^\circ\text{C}$  for 8 h.

In present reaction system,  $\text{Co}^{2+}$  would coordinate with complexing agent (triethylenetetramine or EDTA) to form a complex, which would be reduced to Co with  $\text{N}_2\text{H}_4$ . The reactions could be formulated as follows:



After reaction, the as-prepared film was rinsed with double-distilled water and ethanol alternately, and finally dried in vacuum oven at 50  $^\circ\text{C}$  for 6 h. To obtain nanostructured Co films with different micro-morphology, we altered the synthetic conditions based on our design, which were listed in Table 1.

### 2.2. Characterization

X-ray diffraction (XRD) patterns were recorded using a Shimadzu XD-3A X-ray diffractometer with Cu  $K\alpha$  radiation ( $\lambda = 1.5406 \text{ \AA}$ ). The micromorphology of the film samples were studied using a Hitachi S-4800 field emission scanning electron microscope (FE-SEM). Transmission electron microscopy (TEM)

**Table 1**  
Synthesis conditions and the mass of Co layer of different samples.

Sample name	Complexant/dosage (mmol)	Surfactant/dosage (mmol)	Component of mixed solvent (W:E:G) <sup>b</sup>	Reaction temperature ( $^\circ\text{C}$ )	Mass of Co deposited on Cu substrate (g) <sup>c</sup>
A	Triethylenetetramine/4	/ <sup>a</sup>	40:40:0	100	0.075
B	Triethylenetetramine/4	Sodium dodecylsulfate/4	40:40:0	100	0.086
C	EDTA/4	/	40:20:20	140	0.091

<sup>a</sup> No surfactant was used in the synthesis.

<sup>b</sup> W:E:G denotes the volume ratio of water to ethanol to glycol in the mixed solvent with total volume of ca. 80 mL.

<sup>c</sup> The mass of Co deposited on the Cu foil was determined by calculating the mass difference of the Cu foil before and after deposition reaction.

images were obtained on a Tecnai G2 F30 transmission electron microscope.

### 2.3. Catalytic performance testing

The catalytic hydrolysis of  $\text{NaBH}_4$  was carried out at 25 °C in a glass reactor connected with a gas burette to measure the accumulative volume of  $\text{H}_2$  generated during  $\text{NaBH}_4$  hydrolysis reaction. In a typical procedure, 25 mL of fresh-prepared  $\text{NaBH}_4$  solution (0.2 mol/L) and 25 mL of NaOH solution (0.4 mol/L) was mixed in the reactor, followed by addition of a piece of  $2.5 \times 3$  cm Co film cut from the as-prepared film. To evaluate the reusability of film catalyst, we have repeated the catalytic reaction 10 times with the same catalyst (The reaction time for each catalytic reaction run was 60 min). Typically, after the first run of reaction, the film catalyst was collected and washed thoroughly with double-distilled water and dried in vacuum oven at 50 °C for 4 h. The recovered catalyst was then used in the second run of reaction. The reusability experiment of the reaction was checked up to 10 times in similar model.

## 3. Results and discussion

The Cu foil used in our synthesis is originally purple color and turns to black after reaction, implying that Co has been successfully deposited on the Cu substrate with the assistance of an external magnetic field. The amount of Co deposited on the Cu substrate was determined by calculating the mass difference of the Cu foil before and after deposition reaction, and result is shown in Table 1.

The crystal structures of the film samples, as well as Cu foil, are determined by XRD and results are shown in Fig. 1. Cu foil substrate shows three peaks at  $2\theta = 43.3^\circ$ ,  $50.6^\circ$ ,  $74.2^\circ$ , which can be indexed as face-centered cubic (fcc) phase Cu (PDF#892838). Besides the characteristic peaks of fcc phase Cu, some weak peaks at around  $2\theta = 41.7^\circ$ ,  $44.4^\circ$ ,  $47.5^\circ$ ,  $76.1^\circ$  can be seen in the XRD patterns of the Co films, corresponding to the diffractions from the (100), (002), (101) and (110) planes of hexagonal close-packed (hcp) phase Co (PDF#894308). Notably, the relative intensity of the peaks corresponding to (101)/(100) and (101)/(002) planes of all these sample is much lower than the standard value in JCPDS card (above 3.5), giving a hint that the growth of (101) plane is significantly retarded during the crystal growth and two dimensional nanostructures, such platelets and sheets, may be obtained [29]. To further assess

the preferred growth orientation of Co crystals in the films, the texture coefficient (TC) of different crystal facets are calculated according to the following equation [30]:

$$TC_{(hkl)} = \frac{I_{(hkl)}/I_{0(hkl)}}{\sum I_{(hkl)}/I_{0(hkl)}} \times 100\%$$

where  $I_{(hkl)}$  and  $I_{0(hkl)}$  are the measured diffraction intensity of (hkl) plane of our Co samples and the standard diffraction intensity of (hkl) plane taken from the JCPDS data. The values of TC of different crystal facets of our sample are listed in Table 2, implying that (110) direction is the preferred growth orientation for sample A, while both (110) and (002) directions are the preferred growth orientation for sample B and C. In addition, sample A has the largest  $TC_{(110)}$  among three samples, indicating that sample A has the largest amount of Co crystallites oriented at (110) direction.

The surface morphology of the as-prepared Co film, as well as the Cu foil, is examined by FE-SEM and the results are shown in Fig. 2. The surface of Cu foil is very smooth while that of Co films is rather coarse, indicating that the micro-morphology of the surface of the films has changed significantly. Fig. 2a, b and c indicates that sample A is full of numerous two-dimensional Co nanoplatelets with a thickness of 50–100 nm. It is interesting to note that the surface of these nanoplates is quite coarse and filled with small Co nanosheets with a thickness of less than 10 nm. The synthesis condition of sample B is similar to that of sample A except that the surfactant, sodium dodecylsulfate (SDS), is used in the synthesis. As shown in Fig. 2d, e and f, Co layer in sample B consists of two-dimensional Co nanosheets with a thickness of ca. 10 nm. This suggests that SDS plays a crucial role in decreasing the thickness of nanoplatelets and results in the formation of thin Co nanosheets. Fig. 2g, h and i indicates the Co layer in sample C is comprised of Co microspheres with a typical diameter of hundreds of nanometers, which are made up of Co nanosheets with a thickness of less than 10 nm. TEM analysis is also carried out to confirm the nanostructures of the film and the results are shown in Fig. 2. Compared with those traditional Co thin films composed of nanoparticles, the Co films supported on foil display novel architectures.

The catalytic behaviors of different Co film samples in the hydrolysis reaction of sodium borohydride are assessed and the results are shown in Fig. 3. Firstly, we check the catalytic activity of bared Cu foil. It is found that rate constant in the presence of bared Cu foil is about  $0.165 \text{ mL min}^{-1}$ , demonstrating Cu foil used in our study has nearly no catalytic activity to  $\text{NaBH}_4$  hydrolysis. In contrast,  $\text{H}_2$  generation rates increase significantly in the presence of Co films supported on Cu foil as catalysts. Noting that the accumulative volume of  $\text{H}_2$  generated during  $\text{NaBH}_4$  hydrolysis increases linearly as the reaction time, implying the hydrolysis reaction follows the pseudo-zero order kinetics. The rate constant is  $9.52 \text{ mL min}^{-1}$  for sample A,  $7.22 \text{ mL min}^{-1}$  for sample B and  $6.38 \text{ mL min}^{-1}$  for sample C, respectively. Considering the apparent area of each film catalyst used in catalytic reaction is  $7.5 \text{ cm}^2$ , the rate constant is  $1.27 \text{ mL min}^{-1} \text{ cm}^{-2}$ ,  $0.96 \text{ mL min}^{-1} \text{ cm}^{-2}$  and  $0.85 \text{ mL min}^{-1} \text{ cm}^{-2}$ , respectively. The catalytic activities of our films are much higher than those of the recently reported Co catalyst on the nano-PPX films (the highest rate constant is ca.  $0.36 \text{ mL min}^{-1} \text{ cm}^{-2}$  [18] and  $0.66 \text{ mL min}^{-1} \text{ cm}^{-2}$  [19],

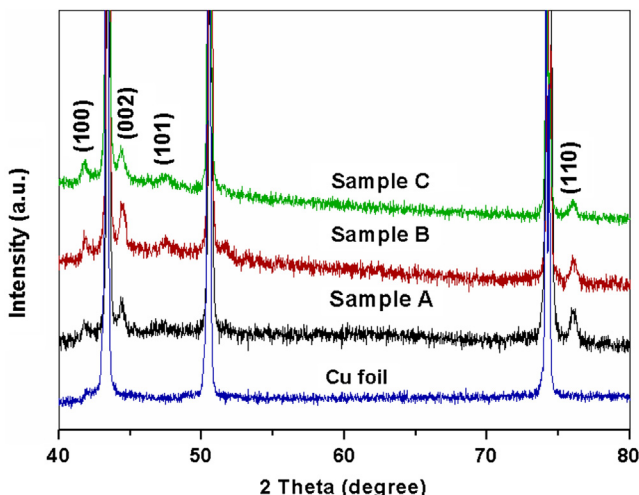
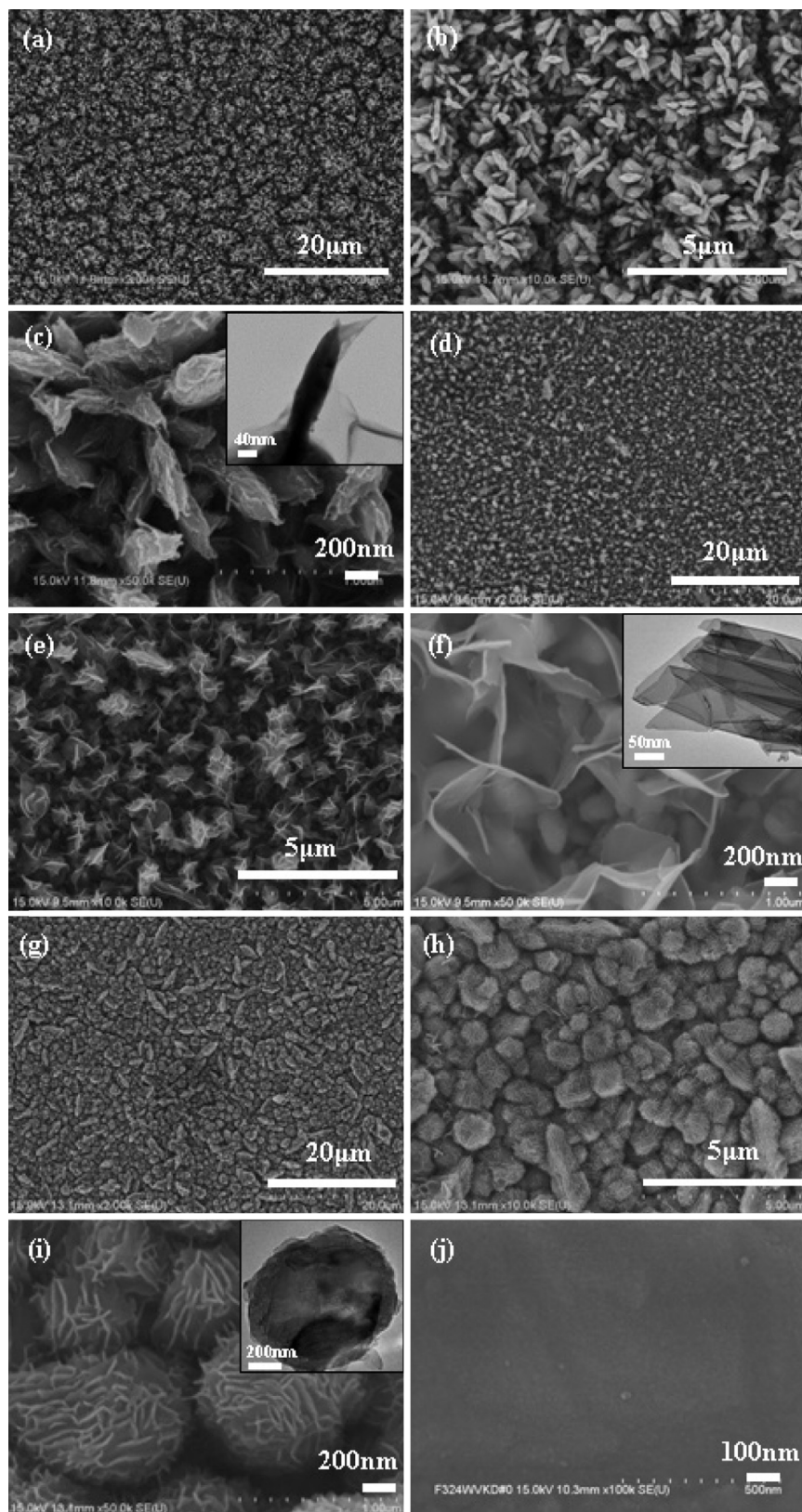


Fig. 1. XRD patterns of Cu foil and different Co films.

Table 2

The texture coefficients of various crystal facets of sample A, B and C.

	$TC_{(100)}$	$TC_{(002)}$	$TC_{(101)}$	$TC_{(110)}$
Sample A	11.1%	18.8%	2.1%	68.0%
Sample B	14.5%	28.1%	2.3%	55.1%
Sample C	13.6%	31.4%	1.2%	53.8%



**Fig. 2.** SEM images of sample A (a, b, c), sample B (d, e, f), sample C (g, h, i) and Cu foil (j). TEM images of sample A, B and C are inseted in c, f, i, respectively.

respectively). It is believed that the shape-anisotropic nanocatalysts with more edges, corners and faces can provide more active sites for catalytic process, which are highly desired in many catalytic reactions. In this study, the as-prepared nanostructured Co

films are severally composed of well-defined nanoplatelets, nanosheets and submicro-spheres consisting of nanosheets, which are expected to exhibit superior catalytic activity to those films consisting of spherical nanoparticles or irregular nanostructures. To

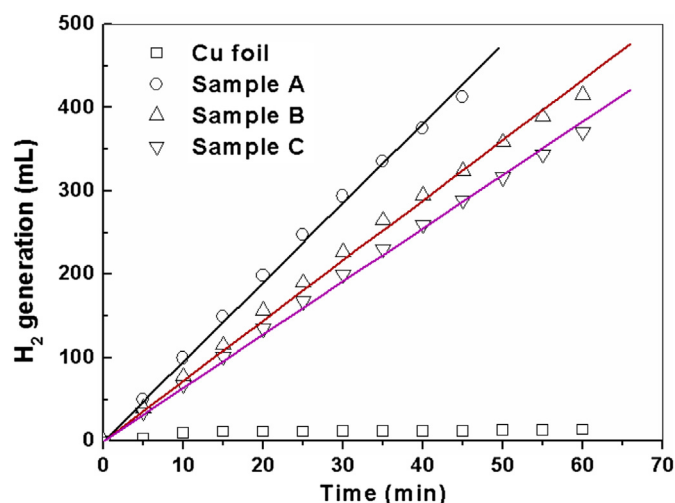


Fig. 3. Hydrogen evolution in the absence of catalyst and in the presence of different Co film catalysts ( $T = 25\text{ }^{\circ}\text{C}$ ,  $C_{\text{NaOH}} = 0.2\text{ mol L}^{-1}$ ).

illustrate this, we carry out a contrast experiment, in which Co film comprised of Co nanograins with a diameter of 100–200 nm (SEM image shown in Fig. 4) is used as catalyst while the other conditions are kept unchanged. It is found that rate constant of Co film comprised of Co nanograins is only  $3.41\text{ mL min}^{-1}$ , implying that the novel and uniform nanostructures in sample A, B and C are responsible for their high catalytic performance. On the other hand, among these three samples, sample A exhibits the best catalytic activity. Two possible reasons account for that observation. The first one is related to the fact that different crystal facets of catalysts have different surface energy and the catalytic activity of a specific facet of catalysts is closely associated with their surface energy in many processes [31,32]. Among the (100), (002), (101) and (110) facets of hexagonal closed-packed Co, (110) facet has the highest surface energy [33]. As shown in Table 2, the percentage of (110) facet of sample A is the largest among these three samples. It is possible that the relatively large ratio of high energy (110) facet brings about a superior catalytic activity to sample A. The second reason can be ascribed to the unsmooth surface on the nanoplatelets of sample A (as shown in Fig. 2c). According to the mechanism of hydrogen generation via  $\text{NaBH}_4$  hydrolysis catalyzed by heterogeneous catalysts [5],  $\text{BH}_4^-$  is adsorbed on the surface of metal

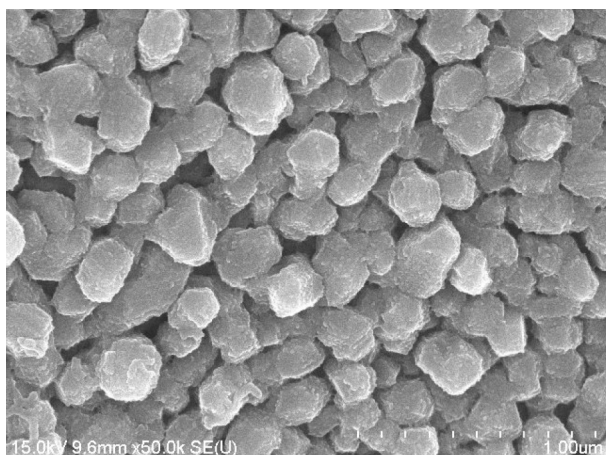


Fig. 4. SEM image of Co film composed of Co nanograins.

catalysts at first and then metal catalyst will transfer electrons to the molecular  $\text{H}_2\text{O}$  to generate hydrogen. Therefore, the rough-surfaced nanoplatelets in the sample A, which is favorable for seizing  $\text{NaBH}_4$  on its surface, is highly desirable [34].

Generally, catalytic hydrolysis of  $\text{NaBH}_4$  is performed in basic solution to avoid the self-hydrolysis of  $\text{NaBH}_4$  and the  $\text{H}_2$  generation rate is highly related to the alkalinity of the reaction medium [2,3,9]. In the present study, hydrolysis of  $\text{NaBH}_4$  in the presence of different Co film catalysts at NaOH concentration ranging from 0.1 to  $1\text{ mol L}^{-1}$  is carried out to determine the optimum hydrolysis condition. As can be observed in Fig. 5,  $\text{H}_2$  generation rate firstly increases and then decreases with the increasing NaOH concentration for sample A and C, which is indicative of an optimum NaOH concentration of  $0.4\text{ mol L}^{-1}$ . In contrast,  $\text{H}_2$  generation rate will increase as the increase of NaOH concentration in the range from 0.1 to  $1\text{ mol L}^{-1}$  for sample B. Notably, the  $\text{H}_2$  generation rate is the most sensitive to the NaOH concentration in the presence of sample C as a catalyst. Increase of NaOH concentration from 0.1 to  $0.4\text{ mol L}^{-1}$  will result in the increase of  $\text{H}_2$  generation rate from  $4.8\text{ mL min}^{-1}$  to  $11.1\text{ mL min}^{-1}$  for sample C.

To investigate the effect of temperature on the  $\text{H}_2$  generation rate,  $\text{NaBH}_4$  hydrolysis was also carried out at temperature of 35, 45, and  $55\text{ }^{\circ}\text{C}$ , the results are shown in Fig. 6. As can be observed, there is a remarkable increase in the  $\text{H}_2$  generation rate with the increase in reaction temperature for all three samples. For example, when sample A acts as catalyst, it will take ca. 45 min to generate  $410\text{ mL H}_2$  at  $25\text{ }^{\circ}\text{C}$ , while it will take only ca. 15 min to produce the same amount of  $\text{H}_2$  at  $55\text{ }^{\circ}\text{C}$ . According to the classical Arrhenius equation, the apparent activity energy ( $E_a$ ) can be figured out based on the data of reaction rates at different temperature (Fig. 6d), which is  $28.4\text{ kJ mol}^{-1}$  for sample A,  $27.6\text{ kJ mol}^{-1}$  for sample B and  $34.3\text{ kJ mol}^{-1}$  for sample C. All these three values are much lower than the  $E_a$  of spontaneous hydrolysis of  $\text{NaBH}_4$  (ca.  $100\text{ kJ mol}^{-1}$  [17]). They are also lower than the  $E_a$  values of the  $\text{NaBH}_4$  hydrolysis catalyzed by different Co catalysts, including bulk Co ( $75\text{ kJ mol}^{-1}$  [9]), Raney Co ( $53.7\text{ kJ mol}^{-1}$  [35]), Co supported on activated carbon ( $44\text{ kJ mol}^{-1}$  [36]), PVP-stabilized Co nanoclusters ( $37 \pm 2\text{ kJ mol}^{-1}$  [9]) and Co nanoparticles ( $35\text{ kJ mol}^{-1}$  [37] and  $38\text{ kJ mol}^{-1}$  [38]). The relatively low  $E_a$  is crucial for the high activity of our film catalysts.

Besides the catalytic activity, the durability and reusability are another important concern for a catalyst from the viewpoint of

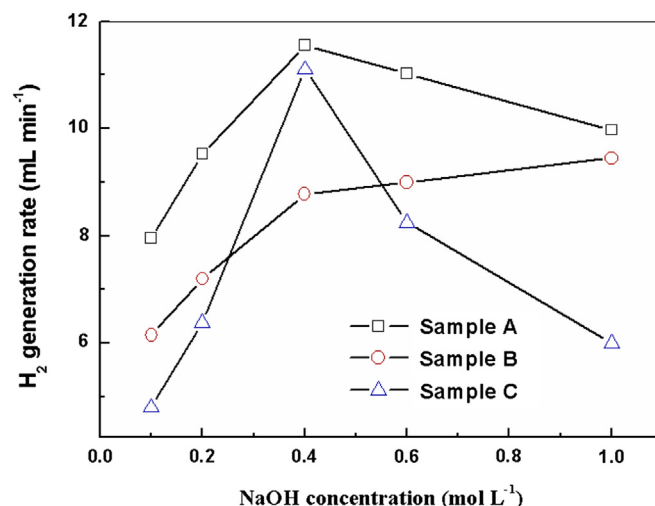


Fig. 5. Hydrogen evolution at different NaOH concentration ( $T = 25\text{ }^{\circ}\text{C}$ ).

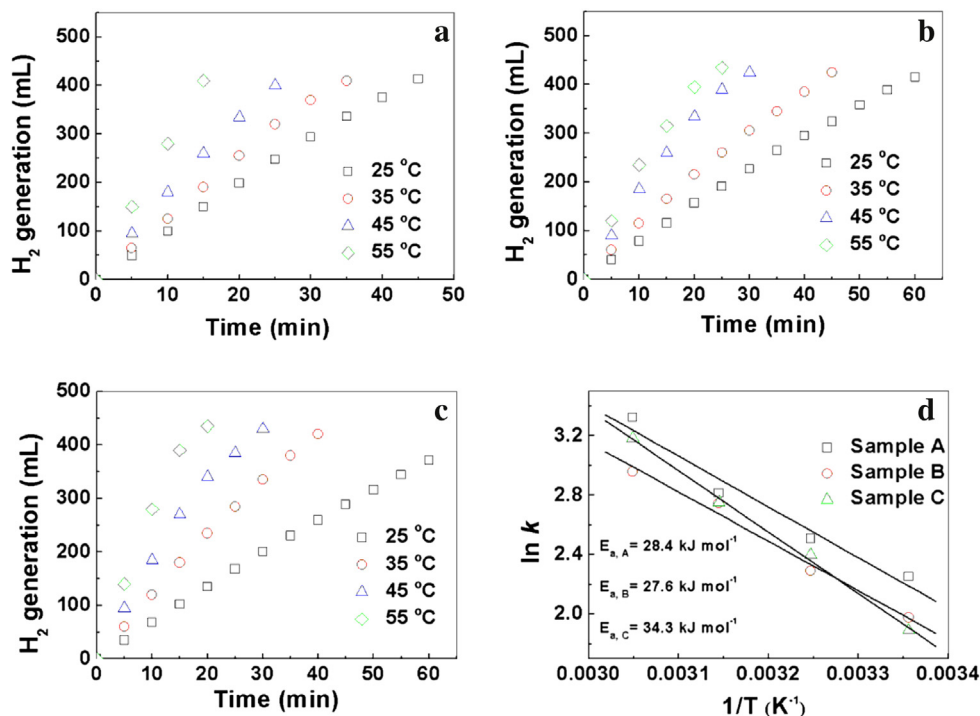


Fig. 6. Hydrogen evolution in the presence of sample A (a), sample B (b), sample C (c) at different temperature and the determination of apparent activation energy in the temperature range from 25 to 55 °C (d) ( $C_{\text{NaOH}} = 0.2 \text{ mol L}^{-1}$ ).

practical application. In the present study, the durability and reusability of a representative Co film, viz. sample A, in the catalytic hydrolysis of  $\text{NaBH}_4$  is assessed by repeating the hydrolysis reaction at 25 °C 10 times. In each cycle, the rate constant was calculated by linear regression analysis of the kinetic data, similar to that shown in Fig. 3.  $k_1$  and  $k_n$  are the rate constant of the reaction in No. 1 and No.  $n$  cycle, respectively. So,  $k_n/k_1$  can be indicative of the loss of catalytic activity of film catalyst in different cycles. Fig. 7 displays the ratio of the rate constant in the different cycle ( $k_n$ ) to that in the first cycle ( $k_1$ ). As can be seen, the film catalyst retains ca. 90% activity of its virginal activity after 10 cycles. In contrast, the recently reported hydroxyapatite-supported Co nanoclusters loses 19% activity after

5 cycles [39], Co/Ni catalyst (Co over Ni foam) loses most of its catalytic activity after 3 cycles [11] and the Co/PCM catalyst shows around 32% catalytic activity loss after 2 cycles [17]. Compared with those Co catalysts in the literature, our film catalyst exhibit significantly improved durability and reusability. A very common reason for the deactivation of nanocatalysts is the aggregation and/or damage of nanostructures of the catalysts during catalytic reactions [32,40]. Fig. 8 displays the SEM image of sample A after 10 reaction cycles. By comparing Fig. 3c with Fig. 8, it is clear that the nanostructures of the used film catalyst don't suffer from destruction, suggesting that the nanostructures in sample A are very stable against aggregation and destruction under our experiment conditions.

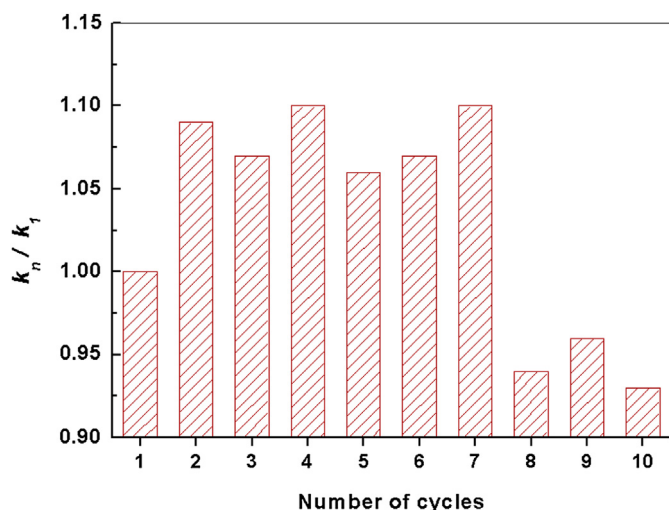


Fig. 7. Normalized rate constant in different cycles ( $T = 25 \text{ °C}$ ,  $C_{\text{NaOH}} = 0.2 \text{ mol L}^{-1}$ ).

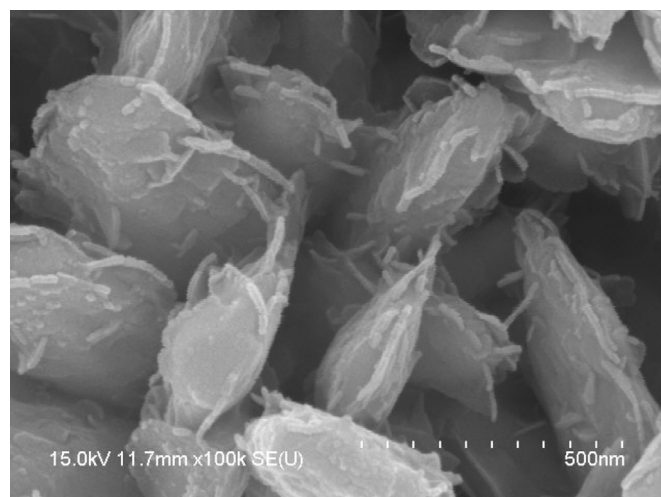


Fig. 8. SEM image of sample A after 10 successive cycles ( $T = 25 \text{ °C}$ ,  $C_{\text{NaOH}} = 0.2 \text{ mol L}^{-1}$ ).

#### 4. Conclusions

In summary, nanostructured Co films supported on the Cu foil substrate were prepared by a facile and cost effective external magnetic-field-assisted deposition route. Compared with those common Co film catalysts consisting of small spherical Co grains, the as-prepared nanostructured Co films were comprised of shape-anisotropic Co nanocrystals, such as Co nanoplatelets, Co nanosheets, and Co microspheres composed of nanosheets. It was found that those nanostructured Co film catalysts exhibited high performance in the hydrolysis of sodium borohydride. The rate constant/apparent activation energy of  $\text{NaBH}_4$  hydrolysis in the presence of different Co film catalysts was  $1.27 \text{ mL min}^{-1} \text{ cm}^{-2}/28.4 \text{ kJ mol}^{-1}$ ,  $0.96 \text{ mL min}^{-1} \text{ cm}^{-2}/27.6 \text{ kJ mol}^{-1}$  and  $0.85 \text{ mL min}^{-1} \text{ cm}^{-2}/34.3 \text{ kJ mol}^{-1}$ , respectively. It was also found that the Co film catalyst composed of nanoplatelets showed only ca. 10% catalytic activity loss after 10 cycles, which exhibited much improved reusability and durability in contrast to those Co catalysts reported in the literature.

#### Acknowledgments

This work was supported by the National Natural Science Foundation of China (No. 51001052, 21163018), the Natural Science Foundation of Guangdong Province (No. 10451601501005315), the Science & Technology project of Huizhou City (2010B020008017), the National Nature Science Foundation of Huizhou University (2012QN07) and the research fund of the Key Laboratory of Fuel Cell Technology of Guangdong Province.

#### References

- [1] A.M.F.R. Pinto, D.S. Falcao, R.A. Silva, C.M. Rangel, *Int. J. Hydrogen Energy* 31 (2006) 1341–1347.
- [2] J. Zhu, R. Li, W. Niu, Y. Wu, X. Gou, *J. Power Sources* 211 (2012) 33–39.
- [3] R. Retnamma, A.Q. Novais, C.M. Rangel, *Int. J. Hydrogen Energy* 36 (2011) 9772–9790.
- [4] U.B. Demirci, P. Miele, *Phys. Chem. Chem. Phys.* 12 (2010) 14651–14665.
- [5] B.H. Liu, Z.P. Li, *J. Power Sources* 187 (2009) 527–534.
- [6] A. Chinnappan, H.-C. Kang, H. Kim, *Energy* 36 (2011) 755–759.
- [7] V.I. Simagina, P.A. Storozhenko, O.V. Netskina, O.V. Komova, G.V. Odegova, Y.V. Larichev, A.V. Ishchenko, A.M. Ozerova, *Catal. Today* 138 (2008) 253–259.
- [8] N. Sahiner, O. Ozay, N. Aktas, Erklinger, J. He, *Int. J. Hydrogen Energy* 36 (2011) 15250–15258.
- [9] Önder Metin, S. Özkar, *Energy & Fuels* 23 (2009) 3517–3526.
- [10] J.C. Walter, A. Zurawski, D. Montgomery, M. Thornburg, S. Revankar, *J. Power Sources* 179 (2008) 335–339.
- [11] O. Akdim, U.B. Demirci, P. Miele, *Int. J. Hydrogen Energy* 36 (2011) 13669–13675.
- [12] J. Hannauer, U.B. Demirci, C. Geantet, J.M. Herrmann, P. Miele, *Phys. Chem. Chem. Phys.* 13 (2011) 3809–3818.
- [13] N. Patel, A. Miotello, V. Bello, *Appl. Catal. B103* (2011) 31–38.
- [14] N. Sahiner, S. Butun, T. Turhan, *Chem. Eng. Sci.* 82 (2012) 114–120.
- [15] J.-H. Oh, J.W. Bae, S.-J. Park, P.K. Khanna, K.-W. Jun, *Catal. Lett.* 130 (2009) 403–409.
- [16] S.-J. Park, J.W. Bae, G.-I. Jung, K.-S. Ha, K.-W. Jun, Y.-J. Lee, H.-G. Park, *Appl. Catal. A* 413–414 (2012) 310–321.
- [17] O. Akdim, R. Chamoun, U.B. Demirci, Y. Zaatar, A. Khoury, P. Miele, *Int. J. Hydrogen Energy* 36 (2011) 14527–14533.
- [18] N. Malvadkar, S. Park, M. Urquidí-MacDonald, H. Wang, M.C. Demirel, *J. Power Sources* 182 (2008) 323–328.
- [19] N.A. Malvadkar, K. Sekeroglu, W.J. Dressick, M.C. Demirel, *J. Power Sources* 196 (2011) 8553–8560.
- [20] N. Tian, Z.-Y. Zhou, S.-G. Sun, Y. Ding, Z.L. Wang, *Science* 316 (2007) 732–735.
- [21] H.G. Yang, G. Liu, S.Z. Qiao, C.H. Sun, Y.G. Jin, S.C. Smith, J. Zou, H.M. Cheng, C.Q. Lu, *J. Am. Chem. Soc.* 131 (2009) 4078–4083.
- [22] Y. Zhang, B. Deng, T. Zhang, D. Gao, A.-W. Xu, *J. Phys. Chem. C* 114 (2010) 5073–5079.
- [23] X. Liu, D. Wang, Y. Li, *Nano Today* 7 (2012) 448–466.
- [24] H. Luo, D. Wang, J. He, Y. Lu, *J. Phys. Chem. B* 109 (2005) 1919–1922.
- [25] W. He, P. Gao, L. Chu, L. Yin, Z. Li, Y. Xie, *Nanotechnology* 17 (2006) 3512–3517.
- [26] H. Li, S. Liao, *J. Mater. Chem.* 19 (2009) 5207–5211.
- [27] J.Y. Zheng, Z.L. Quan, G. Song, C.W. Kim, H.G. Cha, T.W. Kim, W. Shin, K.J. Lee, M.H. Jung, Y.S. Kang, *J. Mater. Chem.* 22 (2012) 12296–12304.
- [28] H. Li, J. Liao, Y. Du, T. You, W. Liao, L. Wen, *Chem. Commun.* 49 (2013) 1768–1770.
- [29] H. Li, S. Liao, *J. Phys. D: Appl. Phys.* 41 (2008) 065004.
- [30] W. Zhang, Z. Yu, Z. Chen, M. Li, *Mater. Lett.* 67 (2012) 327–330.
- [31] Z.L. Wang, *J. Phys. Chem. B* 104 (2000) 1153–1175.
- [32] K. Zhou, Y. Li, *Angew. Chem. Int. Ed.* 51 (2012) 602–613.
- [33] J.-M. Zhang, D.-D. Wang, K.-W. Xu, *Appl. Surf. Sci.* 253 (2006) 2018–2024.
- [34] A. Lu, Y. Chen, J. Jin, G.-H. Yue, D.-L. Peng, *J. Power Sources* 220 (2012) 391–398.
- [35] B.H. Liu, Z.P. Li, S. Suda, *J. Alloys Compd.* 415 (2006) 288–293.
- [36] D. Xu, P. Dai, X. Liu, C. Cao, Q. Guo, *J. Power Sources* 182 (2008) 616–620.
- [37] J. Andrieux, D. Swierczynski, L. Laversenne, A. Garron, S. Bennici, C. Goutaudier, P. Miele, A. Auroux, B. Bonnetot, *Int. J. Hydrogen Energy* 34 (2009) 938–951.
- [38] N. Sahinera, O. Ozay, E. Inger, N. Aktas, *Appl. Catal. B* 102 (2011) 201–206.
- [39] M. Rakap, S. Özkar, *Catal. Today* 183 (2012) 17–25.
- [40] A. Ryu, S.-W. Jeong, A. Jang, H. Choi, *Appl. Catal. B* 105 (2011) 128–135.